UNDERSTANDING SPACE WEATHERING OF CARBONACEOUS ASTEROIDS THROUGH H^+ AND HE^+ ION IRRADIATION OF THE MURCHISON METEORITE. D. L. Laczniak[1], M. S. Thompson[1], R. Christoffersen[2], C. A. Dukes[3], S. J. Clemett[2], R. V. Morris[4], and L. P. Keller[4]. [1]Earth, Atmospheric, and Planetary Sciences Department, Purdue University, West Lafayette, IN, 47907 (dlacznia@purdue.edu), [2]Jacobs, NASA Johnson Space Center, Mail Code XI3, Houston, TX 77058, [3]Laboratory for Astrophysics and Surface Physics, University of Virginia, Charlottesville, VA, 22904, [4]ARES, NASA Johnson Space Center, Houston, TX 77058,

Introduction: Airless planetary bodies are subject to space weathering processes such as micrometeoroid bombardment and solar wind irradiation. These processes alter the microstructural, chemical, and optical properties of planetary regoliths and, in turn, complicate interpretations of surface composition from remote sensing data and matching of meteorites to their parent bodies. Unlike lunar and ordinary chondrite materials, space weathering studies of primitive carbonaceous chondrites are still evolving [1]. Investigations that examine the spectral, microstructural, and chemical effects of space weathering on carbonaceous materials are critical for maximizing the scientific return of ongoing and future missions to C-complex asteroids, like the NASA OSIRIS-REx (Bennu) and JAXA Hayabusa2 (Ryugu) missions [2,3]. Here, we present results from our experimental simulation of solar wind weathering on organic-rich, C-complex asteroid surfaces in which we irradiated a slab of the Murchison CM2 chondrite with 1 keV/amu H^+ and He^+ ions.

Methods: Under ultra-high vacuum (10^{-8} Pa), we irradiated two discrete 6 mm x 6 mm regions of a dry-cut Murchison slab. The first region was irradiated with 4 keV He^+ to a total fluence of 1.1×10^{18} ions/cm^2 using a flux of 1.0×10^{13} ions/cm^2/s (~23,000 yr of exposure at Bennu). The second region was irradiated with 1 keV H^+ to a total fluence of 8.1×10^{17} ions/cm^2 using a flux of 1.9×10^{13} ions/cm^2/s (~700 yr of exposure at Bennu). We then characterized unirradiated, H^+-irradiated, and He^+-irradiated surfaces with five analytical techniques. Changes in surface chemistry driven by ion irradiation were observed *in situ* using an X-ray Photoelectron Spectrometer (XPS; PHI Versaprobe) equipped with a monochromatic, scanning X-ray source ($Al_{K\alpha}$: 1486.7 eV) and hemispherical electron-energy analyzer. Visible to near-infrared reflectance spectra (VNIR; 0.35 – 2.50 µm) collected under ambient conditions with a fiber-optic ASD FieldSpec 3 Spectrometer (Malvern Panalytical) were used to evaluate changes in spectral slope, surface albedo, and absorption band strengths. Modifications to organic functional group chemistry were investigated using spectra and spatial maps acquired with two-step laser-desorption mass spectrometry (µL^{2}MS) at the 118 nm photoionization wavelength. Finally, we used a JEOL 2500SE 200 kV field-emission scanning transmission electron microscope (STEM) equipped with an energy dispersive X-ray spectrometer (EDX) to examine the microstructure and composition of six focused ion beam (FIB) cross-sections extracted from matrix material, Mg-rich olivine (~Fo_{99}), and Fe-rich olivine (~Fo_{55}) in the H^+- and He^+-irradiated regions.

Surface Chemistry and Organics Results: XPS analyses show a significant reduction in matrix carbon content (adventitious and intrinsic) from the uppermost ~10 nm of the Murchison sample in response to both H^+- and He^+-irradiation (a ~71% and ~90% reduction, respectively) (Fig. 1A). High-resolution spectra show that ion irradiation also chemically reduces small amounts of Fe^{3+} and Fe^{2+} to metallic iron (Fig. 1B) and removes surface sulfate and sulfite species by preferentially sputtering oxygen atoms.

Data from the µL^{2}MS instrument acquired with 118 nm (VUV) photoionization detects virtually all aliphatic and aromatic species. Summed spectra indicate that He^+-irradiation decreases bulk organic content and H^+-irradiation increases the abundance of some low-molecular-weight free organic species (i.e., not bound as macromolecular assemblages). Also, OH^- and H_2O abundances increase after H^+- and He^+-irradiation.

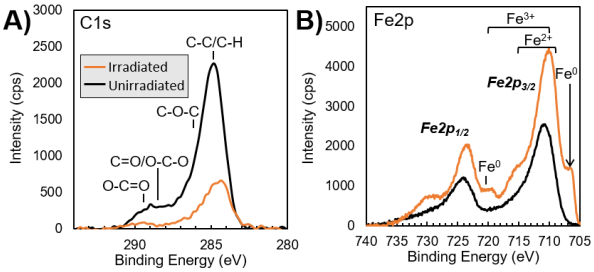

Figure 1. High-resolution XPS spectra of H^+-irradiated matrix material. (A) C1s region showing removal of carbon. (B) Fe2p region showing partial chemical reduction of Fe^{3+} and Fe^{2+}.

VNIR Results: Absolute reflectance spectra suggest that He^+-irradiation causes spectral brightening (increase in albedo) and reddening (increasing reflectance with increasing wavelength) longwards of 0.65 µm while H^+-irradiation causes only minor reddening. Although He^+-irradiation induces greater attenuation, both types of ion irradiation reduce the spectral contrast of the broad absorption between 0.60 and 1.6 µm, which is likely the envelope of bands associated with Fe^{3+} and Fe^{2+} in serpentine group minerals, olivine, and possibly magnetite [4]. Reduced spectral contrast of the ~0.75 µm minimum (Fe^{2+}-Fe^{3+} charge transfer in serpentine/cronstedtite) [4], especially in the He^+-irradiated spectrum, may result from irradiation-driven chemical reduction of Fe^{3+} and

Fe^{2+}.

TEM and EDX Results: TEM analysis of the He^+-irradiated matrix cross-section shows a continuous, highly vesiculated ion-affected layer (~≥100 nm) at the sample's surface (Fig. 2A). High-resolution TEM (HRTEM) images indicate that matrix phyllosilicates are completely amorphous to ~150 nm below the surface. While it is also highly-vesiculated, the ion-affected region of the H^+-irradiated matrix cross-section is thinner, ranging from 40-60 nm (Fig. 2B), and phyllosilicate amorphization reaches a depth of ~65 nm below the surface. Nanoparticles were identified only in the He^+-irradiated matrix sample, both within and below the ion-affected region.

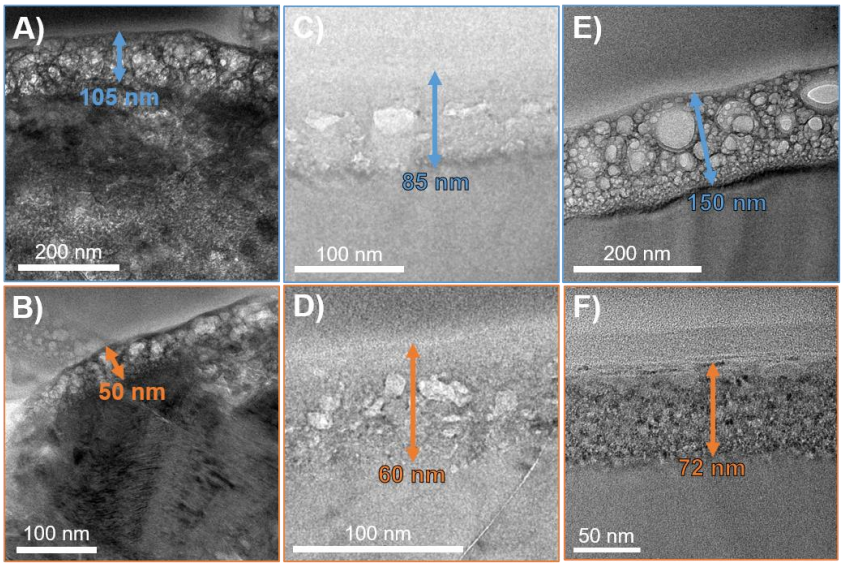

Figure 2. Conventional TEM images of (A) He^+-irradiated matrix, (B) H^+-irradiated matrix, (C) He^+-irradiated Mg-rich olivine, (D) H^+-irradiated Mg-rich olivine, (E) He^+-irradiated Fe-rich olivine, and (F) H^+-irradiated Fe-rich olivine. Arrows indicate thicknesses of ion-affected regions. For clarity, blue labels correspond to the He^+-irradiation experiment and orange labels correspond to the H^+-irradiation experiment.

The ion-affected regions of the He^+- and H^+-irradiated Mg-rich olivine cross-sections are 65-85 nm and 50-85 nm thick, respectively (Fig. 2C and 2D), characterized by moderate vesiculation, and contain both amorphous and polycrystalline material. The He^+-irradiated sample exhibits a relatively Si-enriched, Mg-depleted surface layer while the H^+-irradiated sample has variable surface composition. Some regions of the H^+-irradiated sample have a Mg-enriched, Si-depleted surface or near-surface region that is occasionally overlain by a layer enriched in Si relative to Mg.

Similar to the matrix samples, the He^+-irradiated Fe-rich olivine cross-section exhibits a highly vesiculated, completely amorphous ion-affected region (120-180 nm thick) (Fig. 2E). Interestingly, the H^+-irradiated Fe-rich olivine cross-section has a ~60-75 nm thick ion-affected region with only minor vesiculation that consists of three microstructurally and chemically distinct zones (Fig. 2F). These zones resemble those observed in some Itokawa olivine and low-Ca pyroxene grains [5,6].

Discussion: Results from this study highlight the potential complexities of solar wind space weathering of carbonaceous materials. The spectral brightening induced by He^+-irradiation may reflect removal of surficial carbon, surface roughening, and/or differences in the chondrule abundance in each analyzed region [e.g., 7-9]. Reddening and absorption band attenuation observed in the He^+- and H^+-irradiated spectra may result from the decomposition of phyllosilicates, partial chemical reduction of Fe^{3+} and Fe^{2+}, and subsequent formation of reduced Fe-bearing amorphous material. Regarding organic content, He^+- and H^+-irradiation have opposing effects. The higher energy and heavier mass of the He^+ ions allow them to destroy organics by breaking carbon bonds and sputtering constituent atoms/molecules, thus reducing bulk organic abundance. Alternatively, H^+-irradiation likely does not change bulk organic content but rather breaks apart large macromolecular species, which cannot be detected by the μL^2ms infrared laser, into smaller molecular fragments that *can* be readily desorbed from the sample's surface and detected by the instrument [8]. Microstructurally, the ion-affected regions of our He^+- and H^+-irradiated cross-sections exhibit varying degrees of vesiculation and structural disorder, even across the same mineral phase. Shadowing, a phenomenon which reduces the effective fluence received by local areas of rough sample surfaces, likely contributes to this variation. Thicknesses of these ion-affected regions tend to exceed estimations made by the SRIM software due to radiation-enhanced diffusion and reduced target density from vesiculation [10]. Similar to space weathered rims of Itokawa particles [e.g., 5,6], the ion-processed regions of our He^+-irradiated Mg-rich olivine, H^+-irradiated Mg-rich olivine, and H^+-irradiated Fe-rich olivine samples are partially amorphous, suggesting that a similar microstructure may be observed in returned regolith grains from Bennu and Ryugu.

References: [1] Pieters C.M. & Noble S.K. (2016) *JGR 121*(10), 1865-1884. [2] Lauretta D.S. et al. (2017) *SSRv 212*, 925-984. [3] Watanabe S. et al. (2017) *SSRv 208*, 3-16. [4] Cloutis E.A. et al. (2012) *Icarus 220*, 586-617. [5] Noguchi T. et al. (2014) *MaPS 49*(2), 188-214. [6] Thompson M.S. et al. (2014) *EPS 66*, 89. [7] Moroz L. et al. (2004) *Icarus 170*(1), 214-228. [8] Thompson M.S. et al. (2020) *Icarus 346*, 113775. [9] Dukes C.A. et al (2015) *SpW Workshop*, Abs 2063. [10] Ziegler J.F. et al. (2008) *SRIM*, Lulu Press.